Benchmarking of 2D and 3D Finite Element Calculations With Dynamic Pulse-Buckling Tests of Cylindrical Shells Under Axial Impact*

E.L. Hoffman, D.J. Ammerman
Sandia National Laboratories

INTRODUCTION

In the design of radioactive material transportation packages there are components, such as the impact limiters, that typically undergo large plastic strains during hypothetical accident testing. Also, in these tests it must be demonstrated that the containment boundary does not buckle. In order to analytically determine the response of the packages, the ability of the analysis tools to address these two issues must be evaluated. To accomplish this evaluation an experimental/computational benchmark problem was developed at Sandia National Laboratories. Because the impact test in the hypothetical accident series is a dynamic event, it was desirable to have the benchmark problem consist of dynamic loading at approximately the same strain rate as that observed in the event. This paper will discuss the development of the benchmark problem, describe the test results, and show a comparison between the test results and several 2D and 3D finite element simulations. More details on the test and analyses can be found in (Hoffman and Ammerman 1995).

DESIGN OF THE BENCHMARK PROBLEM

For the purposes of evaluating nonlinear finite element analysis codes, it was desirable for the benchmark problem to produce large amounts of plasticity and buckling. One type of problem that includes these two behaviors is the generation and collapse of a buckle. Because most radioactive material transportation packages use cylindrical components, a cylinder buckling problem was chosen for the benchmark exercise. To have a true buckling problem with cylindrical geometry, it is necessary to load the cylinder with axial compression. This can be accomplished in two ways – using the weight of the cylinder and high accelerations to initiate the buckle or using added mass with lower accelerations. Because the impact velocity for the hypothetical accident test of radioactive material transportation packages is relatively low (13.1 m/s or 30 MPH) it is easier to get buckle initiation and collapse using added mass. With this alternative there are two methods of

* This work was supported by the U. S. Department of Energy under Contract No. DE-AC04-94AL85000.

applying the acceleration pulse to the cylinder -- dropping the cylinder and added mass together onto a stiff target or dropping the added mass onto the cylinder resting on a stiff target. To ensure the impact direction is aligned with the axis of the cylinder, the tests were performed on a shock frame. Within this frame it is easier to have the cylinder resting on the stiff support and impact it with a falling mass.

The maximum mass that can be used in the load frame chosen for the test is 272 kg (600 lb). This limit, along with the desire to have an impact velocity of 13.1 m/s, is a constraint on the size of the cylinder that can be used as the test article. Other constraints come from the desire to produce cylinder buckling instead of column buckling (limits the length to diameter ratio of the test article) and the desire to have plastic flow buckling, where buckling takes place under sustained plastic flow, instead of elastic buckling (limits the diameter to wall thickness ratio). Using these constraints, a 304-L stainless steel cylinder was designed with a length of 20.3 cm (8 inches), an outside diameter of 10.2 cm (4 inches), and a wall thickness of 0.48 cm (3/16 inch).

To control the boundary conditions, the cylinder was clamped between two stiff carbon steel load platens which were recessed (10.2 cm diameter by 0.32 cm deep recess with a 30-degree chamfer as shown in Figure 2) to ensure alignment and to constrain outward radial movement. This recess makes the response of the test unit less dependent on the friction between the cylinder and the platen. The use of these platens also allowed a load cell to be inserted between the cylinder and the stiff support table. Figure 1 shows a schematic and a photograph of the test setup. A 0.64 cm (1/4 inch) thick felt pad was placed

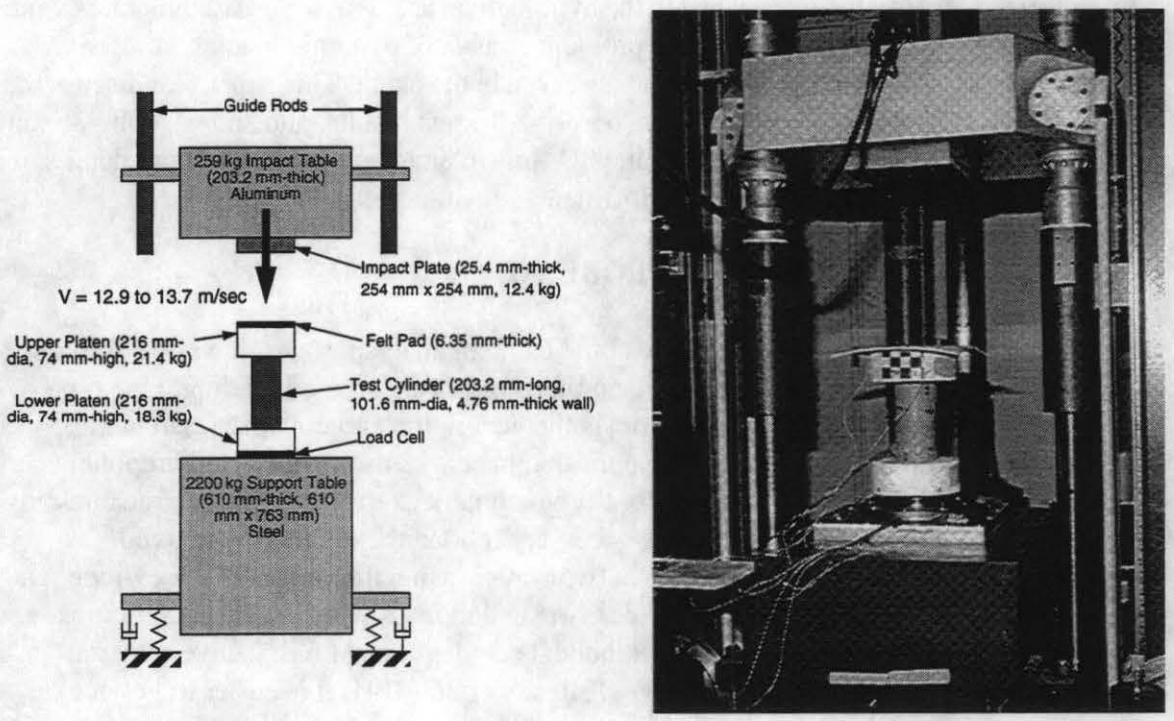

Figure 1. The diagram on the left shows a schematic of the test set-up used for the benchmark tests. The diagram on the right shows a picture of the test setup.

between the impacting mass and the top platen to cushion the impact and prevent damage to the load frame.

A preliminary test with no instrumentation was conducted to determine if the behavior of the test article qualitatively matched the numerical prediction. The impact velocity for this test was 13.0 m/s. The cylinder behaved as expected with four buckles forming along the length of the cylinder. The bottom buckle became unstable and collapsed. This behavior matched the predicted finite element response, so the test series continued.

INSTRUMENTATION

Each of the tests was instrumented to provide data for comparison to the finite element predictions. Accelerometers were placed on the impact table, the top platen, the bottom platen, and the support table. Two accelerometers were used in each location to provide redundant data. Strain gages were also attached to the cylinder to measure surface strains. Axial and hoop gages were installed in each quadrant around the bottom of the cylinder. These gages were used to determine if there are any radial asymmetries in the behavior of the cylinder. In addition, six axial strain gages were installed near the location of the largest buckle at the top of the cylinder. These gages were used to determine the profile of the buckle. Figure 2 shows the location of the instrumentation on the test unit, where labels S1 thru S14 denote strain gages and labels A1 thru A4 denote accelerometers.

TEST RESULTS

Four nominally identical impact tests were conducted in the test series. For each of these tests the impact table was raised to a height above the test unit that had been calibrated to

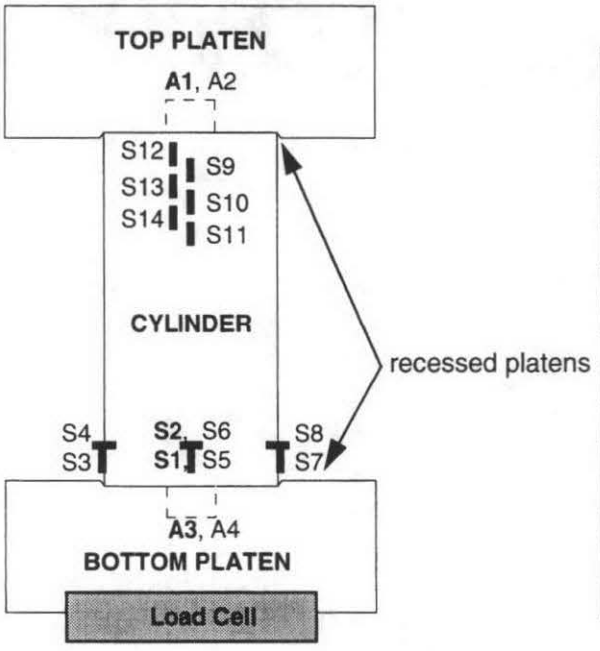

Strain Gage Designation	Location (from bottom)	Direction
S1	0°/0.95 cm	axial
S2	0°/0.95 cm	hoop
S3	90°/0.95 cm	axial
S4	90°/0.95 cm	hoop
S5	180°/0.95 cm	axial
S6	180°/0.95 cm	hoop
S7	270°/0.95 cm	axial
S8	270°/0.95 cm	hoop
S9	0°/19.0 cm	axial
S10	0°/17.8 cm	axial
S11	0°/16.5 cm	axial
S12	0°/19.7 cm	axial
S13	0°/18.4 cm	axial
S14	0°/17.1 cm	axial

Figure 2. Instrumentation on the test unit. In addition, two accelerometers (A5 and A6) are located on the impact table and two (A7 and A8) on the support table.

result in an impact velocity of 13.1 m/s. This height is less than the 9-meters required for a free fall to result in this velocity because the impact table is accelerated downward with elastic ropes. The impact table slides down on two guide tubes that incorporate a braking system to prevent secondary impacts after rebound. Because of slight variations in the friction between the impact table and the guide tubes and the force in the elastic ropes, the impact velocity for the four tests varied from 12.9 m/s to 13.7 m/s. In the first, second, and fourth tests the top buckle became unstable and collapsed, the opposite of what had been seen in the scoping test. In the third test the bottom buckle collapsed. Figure 3 shows the post-test shapes for the four test units. This bi-modality of test results for nominally identical tests was very surprising. However, in each of the tests the accelerations and the loads from the load cell were nearly identical (See Figure 4). Furthermore, the deformed shapes of the two test results, although inverted from top to bottom, were nearly identical. This implies the two results are mechanistically similar.

The large surface strains that occur in the region of the collapsed buckle generally caused the strain gages to fail. However, a measure of the plasticity experienced by the test unit

Figure 3. Deformed shape for the four test articles.

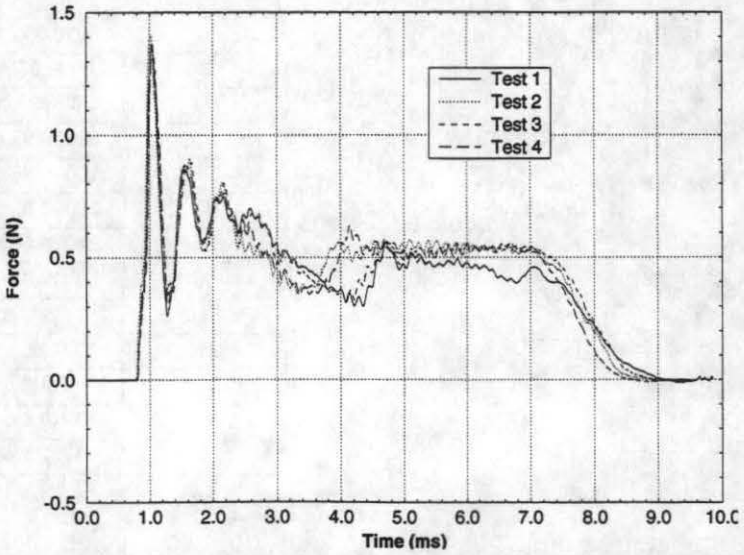

Figure 4. Load vs. time plots from the load cell for all four tests.

can be obtained from the final deformed shape. For each of the test units a profile was made along the outer radius at three circumferential locations to accurately display the deformed shape. Figure 5 shows these profiles for Tests 2 and 4. From the plots it can be seen that the deformed shape of Test 2 was very nearly axisymmetric, while Test 4 exhibited ovaling.

COMPUTATIONAL MODELS

Seven numerical simulations of the pulse buckling test were performed for this study (Hoffman and Ammerman 1995). The 2D and 3D finite element models are shown in Figure 6. The continuum models utilize five constant strain elements through the wall thickness, generally considered an acceptable compromise between accuracy and cost. The simulations were performed using the PRONTO codes (2D and 3D) developed at Sandia National Laboratories (Taylor and Flanagan 1987 and 1989) and ABAQUS/Explicit (Hibbitt et al. 1991), a commercially available code. Both codes are designed for analyzing large deformations of highly nonlinear materials subjected to high strain rates. All four

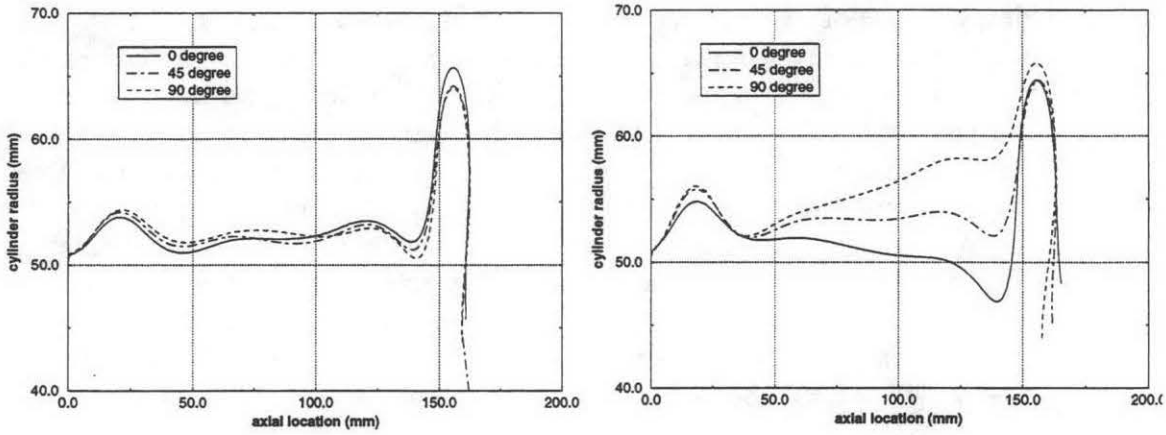

Figure 5. Deformed shape profiles from Tests 2 and 4.

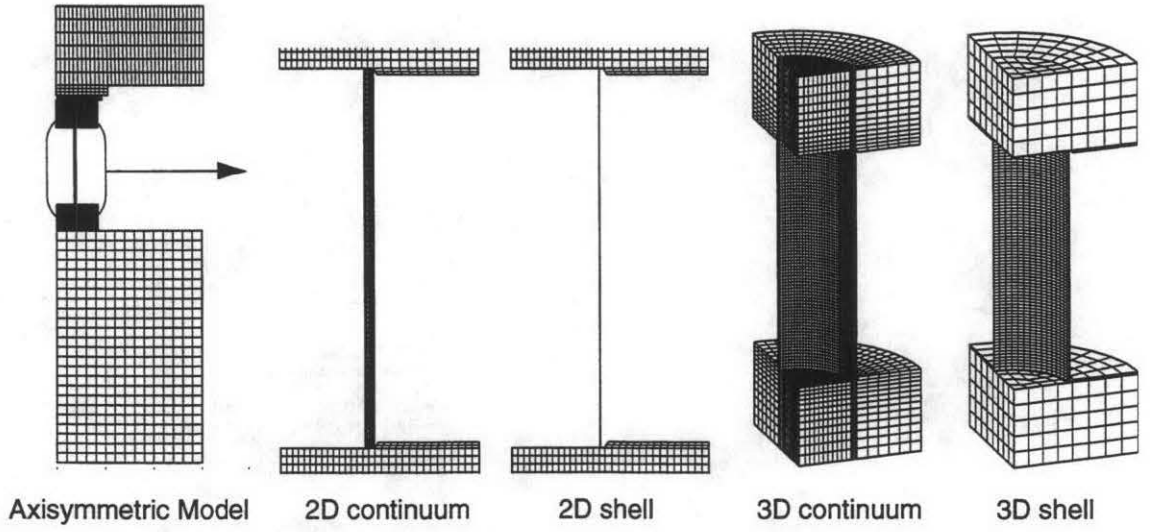

Figure 6. Two and three-dimensional finite element models used in benchmark study.

models were analyzed with ABAQUS/Explicit, while all but the 2D shell model were analyzed with the PRONTO codes (PRONTO2D does not have shell elements). Based on a parametric study of the pneumatic support system of the 2,200-kg support table, it was determined that, for the short duration of the buckling event, the spring forces are negligible compared to the inertial forces and are therefore neglected in the simulations. The 304-L stainless steel test cylinder was modeled using a power law hardening model (Stone et al. 1990) which describes post-yield strain hardening by a power law relationship. To approximate the energy absorption characteristic of the felt pad, it was modeled as a linear-hardening material. All other components were modeled as elastic materials.

ANALYSIS RESULTS

All four of the 3D calculations yielded an axisymmetric buckling pattern. The only way that ovaling could be produced in the analyses was to introduce asymmetries in the boundary conditions. In Figure 7 the seven computed profiles are compared to the profile of Test 2 which buckled nearly axisymmetrically. All of the shell calculations predicted four equally spaced nodes, with one of the end nodes becoming unstable and collapsing. The two smaller buckles in-between the larger buckles are not as evident in the simulations because the cylinder bulges at the middle, making the two smaller buckles appear more like one. However, the smaller buckles are present in all of the shell element calculations as is evident by the correct spacing of the larger buckles. Three buckles would result in the larger buckles being positioned farther from the ends. Like the tests, the shell computations produced two results: one with the buckle on top and one with the buckle at the bottom. In numerical studies, the rebound kinematics of the impact table, and hence the location of the buckling instability, were found to be sensitive to the felt pad properties. However, the two buckled shapes obtained numerically were identical, only inverted top-to-bottom. Hence, the two post-buckled shapes observed in the tests represent mechanistically similar if not identical solutions.

Both of the 3D continuum calculations and the ABAQUS 2D continuum calculation do not agree very well with the test unit. The bending response of the shell walls in these calculations was too stiff, resulting in only three equally spaced buckles. The higher

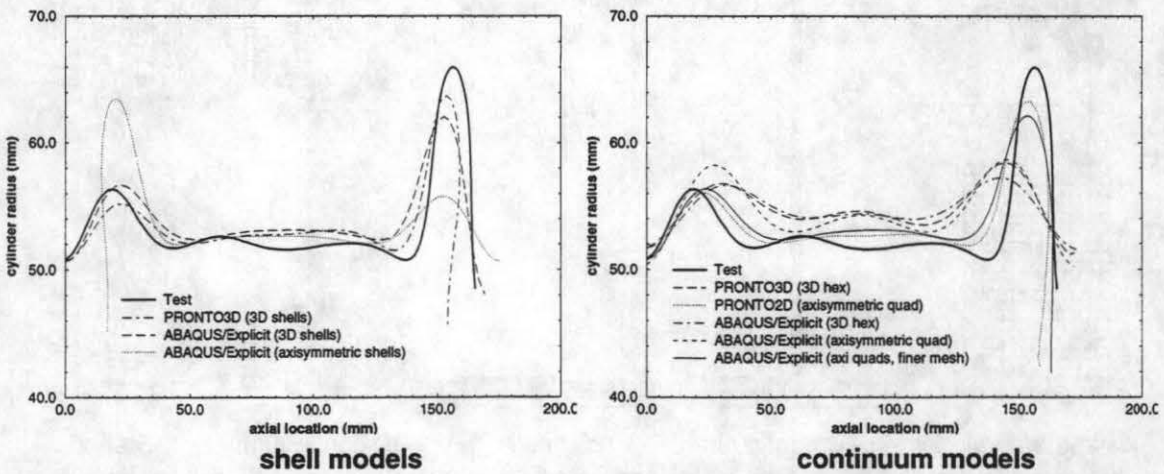

Figure 7. Deformed shape profiles of the shell and continuum element models.

stiffness in these models inhibited the development of the buckling instability. However, the PRONTO2D 2D continuum calculation, using the same mesh refinement as the ABAQUS model, showed good agreement with the test. Also shown in the plot are the results of the ABAQUS 2D continuum calculation run with a finer mesh, using 11 elements through the thickness and 200 along the length (versus 5×75). The results of this calculation compare much more favorably with the test. Hence, five elements through the tube wall thickness is not necessarily adequate for all codes and element types. Neither of the 3D continuum models were run with finer meshes due to computational expense. However, it is reasonable to expect a similar improvement in performance with further mesh refinement.

For the results of finite element simulations to be useful to the cask designer, the codes must be able to correctly predict the dynamic crush force during a buckling event. Figure 8 shows a comparison of the measured load history from Test 1 with that predicted by PRONTO2D using 2D continuum elements. Initial inspection of this plot reveals that the predicted maximum crush force of 0.7 MN differs significantly from the measured maximum of 1.42 MN. However, the measured maximum occurs during the initial load rise and is part of a high amplitude 2,000-Hz component which damps out after several cycles. After this component has damped out (2 ms after impact), the predicted and measured loads show good agreement. To verify the measured load, the output of accelerometer A8 in Test 1 was filtered to 500 Hz and multiplied by the mass of the support table (which is spring mounted), yielding an acceleration-derived crush force which is also plotted in Figure 8. Note that this acceleration-derived load history shows very good agreement with the predicted crush force. Hence, it appears that the load cell data are influenced by instrument response to the shock load. Further evidence of this was observed from accelerometer A3 located on the lower platen, which also exhibited a 2,000-Hz component which damped out after several cycles. Like the felt pad, the load cell can effect the rebound kinematics of the impact table and, hence, the location of the buckling instability.

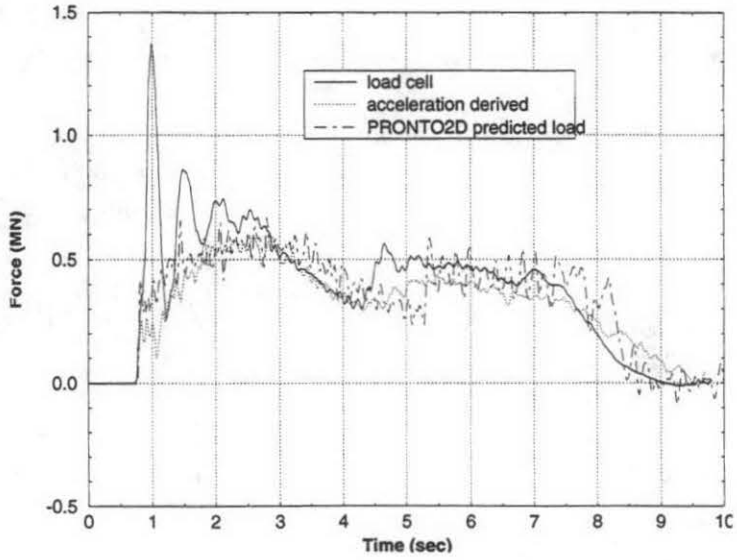

Figure 8. Comparison of the measured and predicted load histories with the load history derived from accelerometer data.

CONCLUSIONS

The results of this study demonstrate the difficulties associated with developing a benchmark problem for numerical code verification. Considerable effort was made to produce a problem with large deformations and boundary conditions which were well defined. Even with this level of concern, the tests produced multiple results due to variations in the boundary conditions and a sensitivity inherent in the design. This sensitivity was also exhibited in the numerical simulations of the event. Several factors in this benchmark problem made comparison with analysis results difficult. The load cell data was affected by the flexibility and dynamic response of this component. Furthermore, the load cell and felt pad could affect the dynamic response of the event (i.e. the location of the buckling instability). The ovaling observed in the tests was an indication of asymmetries in the boundary conditions. Finally, the high strain gradient along the length of the cylinder also made it difficult to predict the strain time-history at a specific location. A small error in the placement of the strain gage can result in a large change in measured strain.

The difficulty associated with designing a controlled test must be taken into consideration whenever test results are being used to benchmark finite element analyses. Often times benchmark problems are based on a single test, and calculations which produce different results from the test are dismissed as being incorrect. By performing multiple tests, the unstable nature of the problem was experimentally confirmed. Even with these difficulties, all of the evaluated codes predicted dynamic buckling without the inclusion of material or geometric imperfections. Although some of the calculations were too stiff, it was demonstrated that improvements in the mesh refinement would improve the accuracy of these predictions. This program demonstrates the ability of the finite element method to determine response to loads similar to those seen by radioactive material transportation package subjected to the hypothetical accident sequence required by regulations.

REFERENCES

Hibbitt, Karlson, and Sorensen, Inc., *ABAQUS/Explicit Users' Manual*, (1991).

Hoffman, E.L., and Ammerman, D.J. *Dynamic Pulse Buckling of Cylindrical Shells under Axial Impact: A Comparison of 2D and 3D Finite Element Calculations with Experimental Data*, SAND93-0350, Sandia National Labs, Albuquerque, NM (1995).

Stone, C.M., Wellman, G.W., and Krieg, R.D. *A Vectorized Elastic-Plastic Power Law Hardening Material Model Including Luders Strain*, SAND90-0153, Sandia National Labs, Albuquerque, NM (1990).

Taylor, L.M., and Flanagan, D.P. *PRONTO2D: A Two-dimensional Transient Solid Dynamics Program*, SAND86-0594, Sandia National Labs, Albuquerque, NM (1987).

Taylor, L.M., and Flanagan, D.P. *PRONTO3D: A Three-dimensional Transient Solid Dynamics Program*, SAND87-1912, Sandia National Labs, Albuquerque, NM (1989).